ONLINE SUPPLEMENT

FORUM ORIGINAL RESEARCH COMMUNICATION

Forum Editor: Andreas Daiber

Molecular mechanisms of the crosstalk between mitochondria and NADPH oxidase through reactive oxygen species – studies in white blood cells and in animal models

Swenja Kröller-Schön[a]*, Sebastian Steven[a]*, Sabine Kossmann[a,b], Alexander Scholz[a], Steffen Daub[a], Matthias Oelze[a], Ning Xia[c], Michael Hausding[a], Yuliya Mikhed[a], Elena Zinßius[a], Michael Mader[a], Paul Stamm[a], Nicolai Treiber[d], Karin Scharffetter-Kochanek[d], Huige Li[c], Eberhard Schulz[a], Philip Wenzel[a,b], Thomas Münzel[a], and Andreas Daiber[a¶]

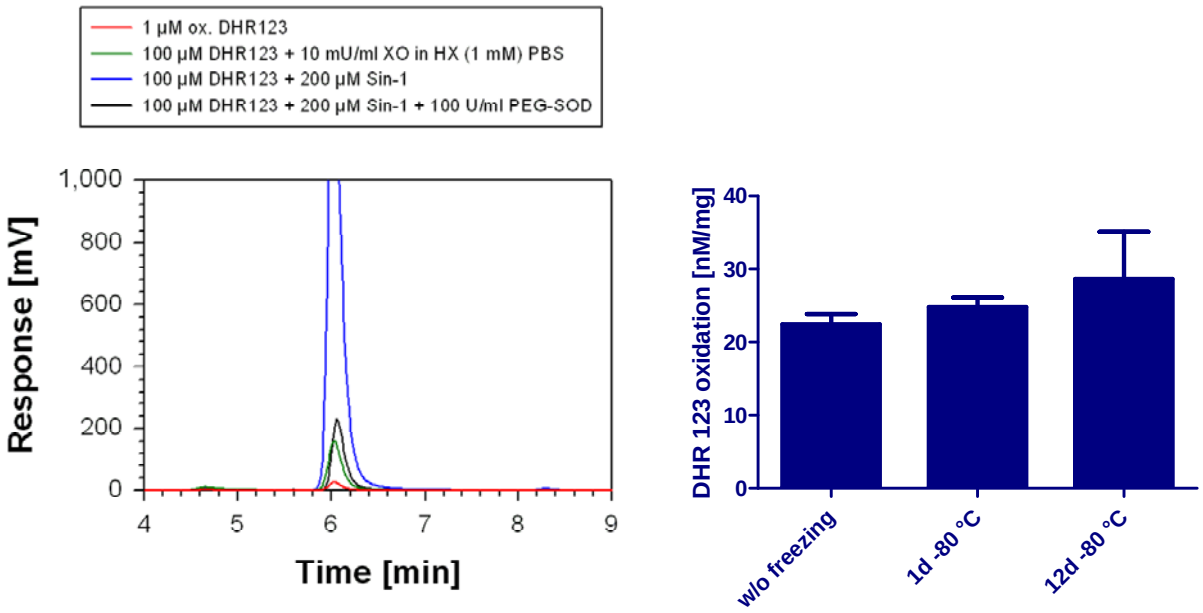

Supplemental Figure S1. HPLC-based detection of oxidized DHR123 as a read-out of cytosolic oxidative stress. The left panel shows representative chromatograms of oxidized, fluorescent DHR123 product, rhodamine. Most efficient oxidation was observed with the peroxynitrite donor Sin-1, which releases simultaneously superoxide and NO. Addition of superoxide dismutase (PEG-SOD) almost completely suppressed the signal indicating that DHR123 does not detect the remaining NO. Also superoxide formation from a xanthine oxidase system using hypoxanthine as a substrate, only generated a minor signal. These data indicate that DHR123 is a sensitive probe for peroxynitrite. The right panel shows data on the stability of the DHR123 oxidation product rhodamine as well as autoxidation of DHR123 in cardiac tissue samples of wild type mice during storage at -80 °C. Comparison of the HPLC-determined rhodamine concentration showed a minor increase between immediately homogenated tissue with subsequent extraction of the oxidized product as compared to work-up after 1 day of storage at -80 °C. However, this increase was not significant but showed a further trend of increase upon 12 days of storage. The data are mean ± SEM of 3 independent experiments.

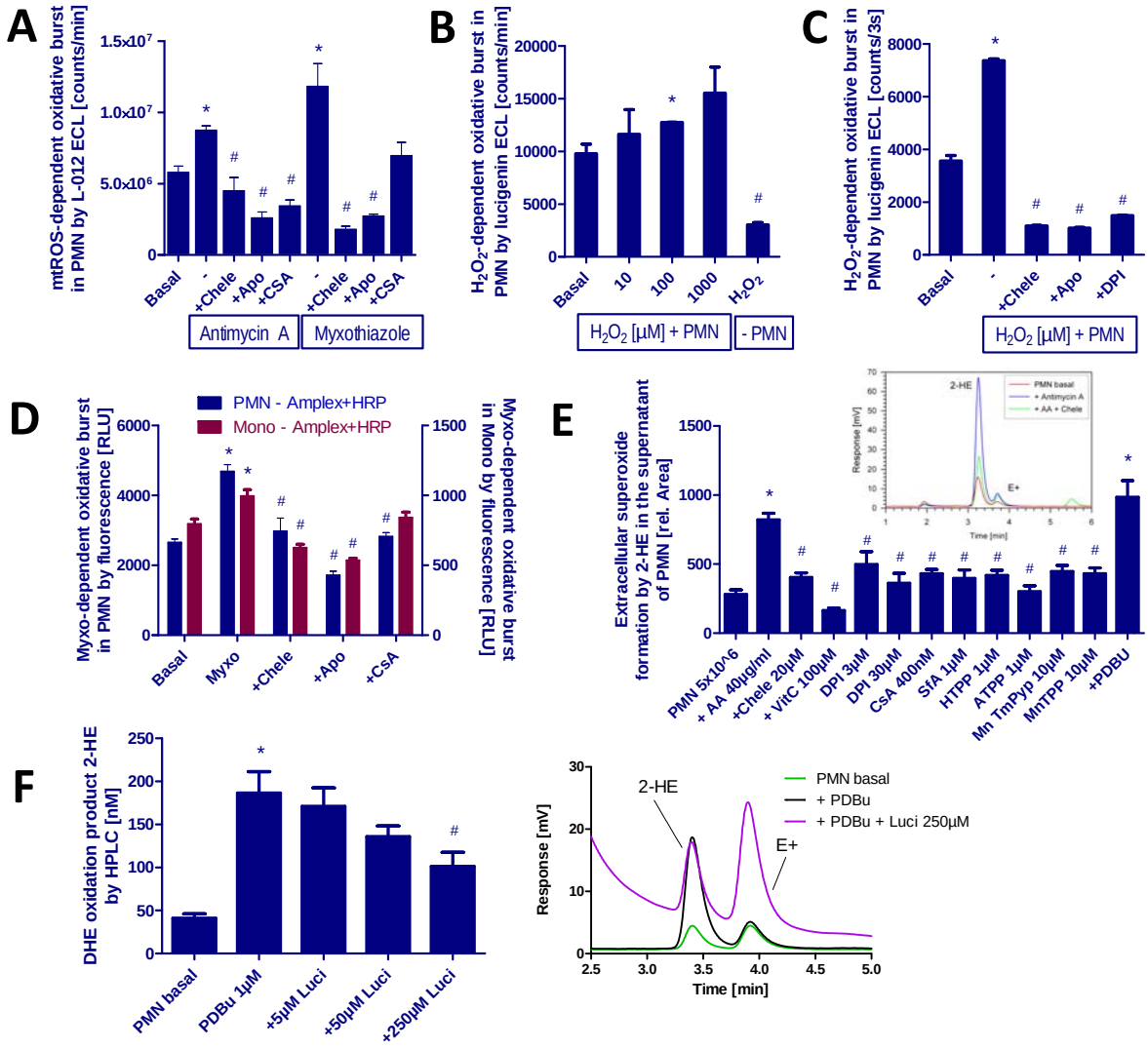

Supplemental Figure S2. Determination of mtROS triggered NADPH oxidase activation in isolated human neutrophils by oxidative burst measurement. (**A**) Antimycin A (20 µg/ml) or myxothiazol (20 µM) stimulated oxidative burst in isolated PMN ($5x10^5$/ml) was determined by L-012 (100 µM) ECL with or without chelerythrine (Chele, 10 µM), apocynin (Apo, 100 µM) or cyclosporin A (CsA, 200 nM). L-012 ECL detects intra- and extracellular ROS and RNS (sensitivity: peroxynitrite > superoxide > hydrogen peroxide). The signal (counts/min) was measured after an incubation time of 20 min with a chemiluminometer (Lumat 9507). (**B** and **C**) Hydrogen peroxide induced oxidative burst in isolated PMN ($5x10^5$/ml) was determined by lucigenin ECL with or without PKC (Chele, 10 µM) or Nox inhibitors (Apo, 100 µM) including diphenylene iodonium (DPI, 100 µM)). Lucigenin ECL detects extracellular superoxide. The signal (counts/min (**B**) or counts/3s (**C**)) was measured after an incubation time of 20 min with a chemiluminometer (Lumat 9507, **B**) or with a chemiluminescence plate reader (Centro 960, **C**). (**D**) Myxothiazol stimulated oxidative burst

in isolated PMN or monocytes/lymphocytes ($5x10^5$/ml) was determined by amplex red (100 µM)/peroxidase (HRP, 0.1 µM) fluorescence with or without PKC, Nox or mPTP inhibitors (same concentrations as in (**A**)). Amplex red is oxidized to resorufin and in the presence of HRP is specific for extracellular hydrogen peroxide (theoretically also peroxynitrite). The signal (RLU) was measured after an incubation time of 30 min with a fluorescence plate reader (Twinkle 970). (**E**) Antimycin A stimulated oxidative burst in isolated PMN ($1x10^6$/ml) upon 20 min of incubation was determined by HPLC-based quantification of 2-hydroxyethidium (2-HE) with or without inhibitors and antioxidants (see list of abbreviations). 2-HE in the supernatant specifically detects extracellular superoxide. (**F**) The effect of increasing lucigenin concentrations on the PDBu–driven superoxide formation in isolated PMN ($1x10^6$/ml) upon 10 min of incubation was determined by HPLC-based quantification of 2-hydroxyethidium (2-HE). Inhibitors were generally preincubated for 5 min. The data are mean ± SEM of 3 (**A-C**), 3-4 (**D**), 3-17 (**E**) and 3 (**F**) independent experiments. *, $p<0.05$ vs. unstimulated control; $^{\#}$, $p<0.05$ vs. stimulated group (antimycin A, myxothiazole or phorbol ester [PDBu]).

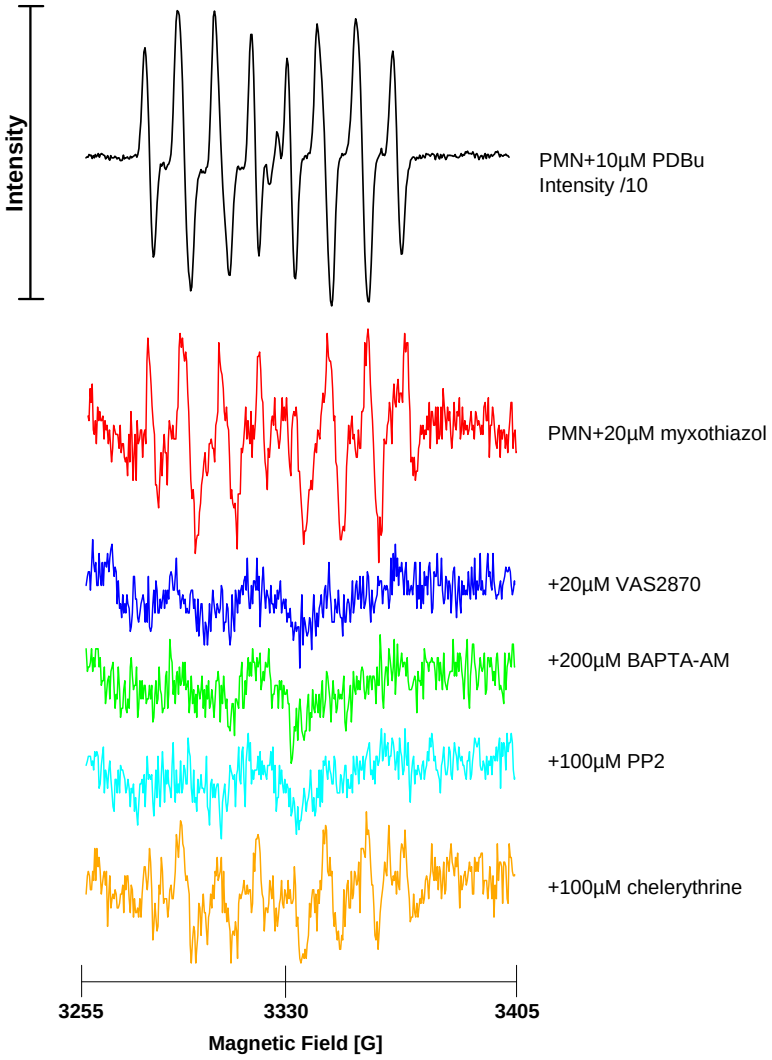

Supplemental Figure S3. Determination of mtROS triggered NADPH oxidase activation in isolated human neutrophils by electron paramagnetic resonance measurement. Freshly isolated human neutrophils ($22x10^6$ PMN/ml) were incubated in PBS with 300 µM Ca^{2+}/Mg^{2+} and 10 mM DEPMPO for 15 min at 37 °C. Activators and inhibitors of phagocytic NADPH oxidase were added as shown in the figure. The spectrum for phorbol ester (PDBu)-stimulated PMN is displayed at decreased intensity (1/10). All reactions below the red spectrum contained 20 µM myxothiazol. Incubations were with Nox inhibitor (VAS2870), intracellular calcium chelator (BAPTA-AM), cSrc kinase inhibitor (PP2) and PKC inhibitor (chelerythrine). All spectra were recorded at room temperature in 50 µl glass capillaries (Hirschmann Laborgeräte GmbH, Eberstadt, Germany). EPR conditions: B_0=3300G, sweep=150G, sweep time=60s, modulation=3000mG, MW power=10 mW, gain=$9x10^2$ using a Miniscope MS200 from Magnettech (Berlin, Germany). Representative spectra of mixed DEPMPO-OOH• and DEPMPO-OH• adduct for 2 independent experiments. Spectra were recorded as described previously (2).

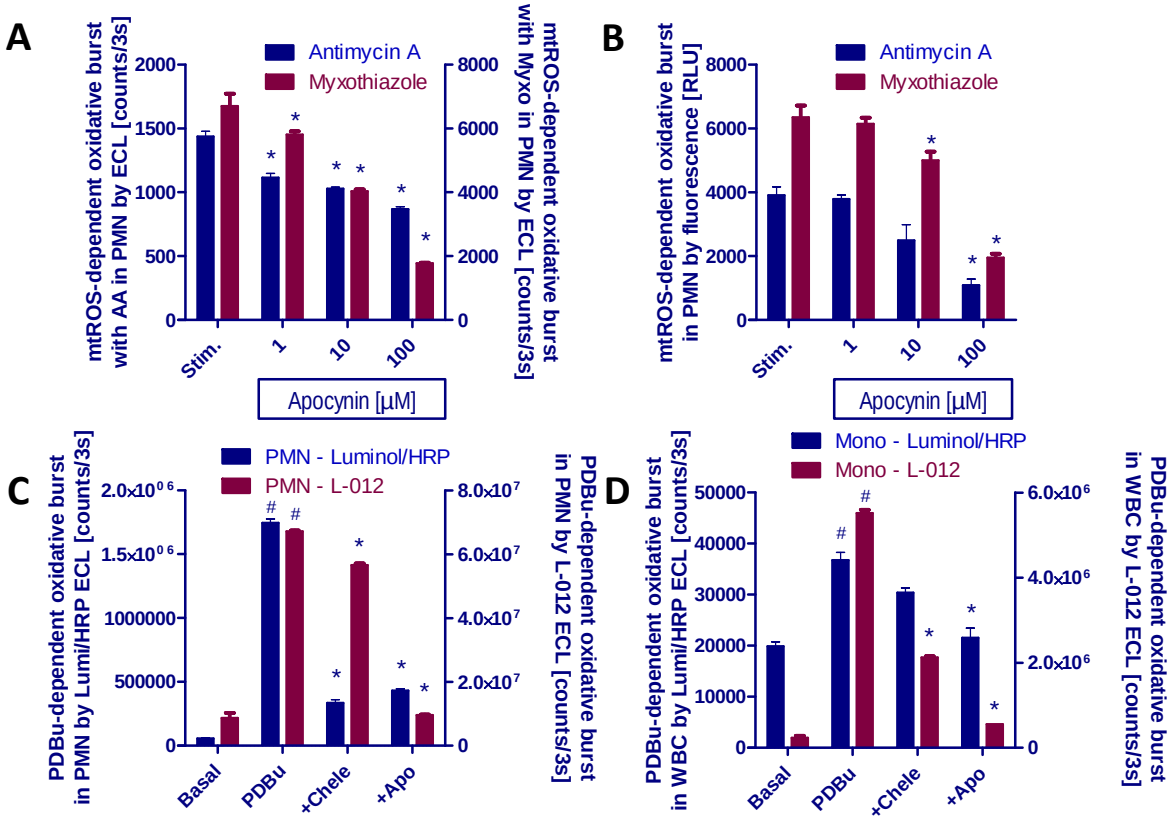

Supplemental Figure S4. Determination of mtROS versus phorbol ester triggered NADPH oxidase activation in isolated human neutrophils by oxidative burst measurement. (**A** and **B**) Antimycin A (20 µg/ml) or myxothiazol (20 µM) stimulated oxidative burst in isolated human PMN ($5x10^5$/ml) was determined by L-012 (100 µM) ECL (**A**) or amplex red (100 µM) / HRP (0.1 µM) fluorescence (**B**) with increasing concentrations of apocynin. L-012 ECL detects intra- and extracellular ROS and RNS (sensitivity: peroxynitrite > superoxide > hydrogen peroxide). The signal (counts/3s) was measured after an incubation time of 30 min with a chemiluminescence plate reader (Centro 960). Amplex red is oxidized to resorufin and in the presence of HRP is specific for extracellular hydrogen peroxide (theoretically also peroxynitrite). The signal (RLU) was measured after an incubation time of 30 min with a fluorescence plate reader (Twinkle 970). (**C** and **D**) PDBu (0.2 µM) stimulated oxidative burst in isolated PMN (**C**) or monocytes/lymphocytes (**D**) ($5x10^5$/ml) was determined by L-012 (100 µM) and luminol (100 µM) / HRP (0.1 µM) ECL. Luminol/HRP ECL mainly detect extracellular hydrogen peroxide. The signal (counts/3s) was measured after an incubation time of 30 min with a chemiluminescence plate reader (Centro 960). The data are mean ± SEM of 4 (**A**-**B**) and 3 (**C** and **D**) independent experiments. *, $p<0.05$ vs. stimulated group (antimycin A, myxothiazole or phorbol ester [PDBu]); $^{\#}$, $p<0.05$ vs. unstimulated group (basal).

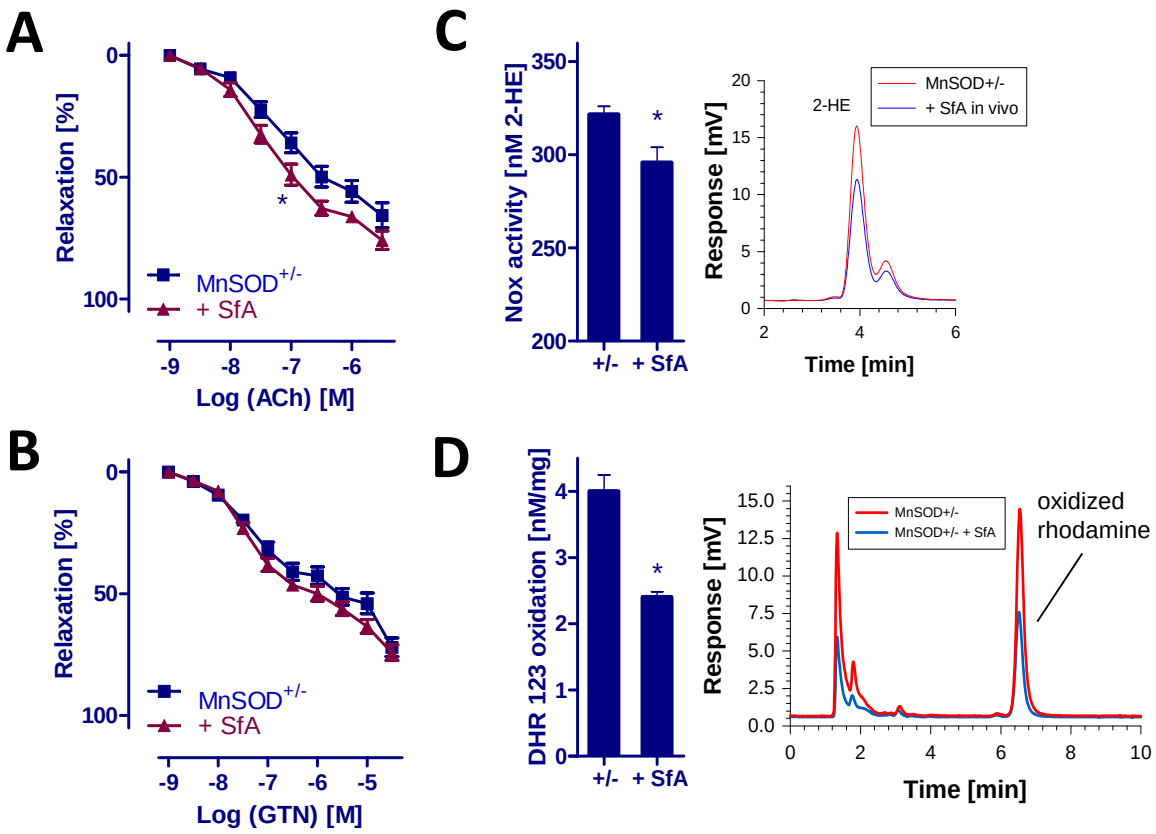

Supplemental Figure S5. Effects of mPTP inhibition by in vivo sanglifehrin A therapy on vascular function and cardiac oxidative stress in old (age: 12 months) MnSOD$^{+/-}$ mice. (**A** and **B**) Vascular function was determined by isometric tension recording and relaxation in aortic ring segments in response to endothelium-dependent (ACh, **A**) and endothelium-independent (nitroglycerin, GTN, **B**) vasodilators. Aorta were used from old MnSOD$^{+/-}$ mice with or without sanglifehrin A (SfA) therapy (10 mg/kg/d). (**C**) Cardiac Nox activity was assessed by HPLC-based quantification of 2-hydroxyethidium (2-HE) in membranous fractions (0.2 mg/ml final protein concentration) from murine hearts in the presence of NADPH (200 µM). This assay is specific for NADPH oxidase-derived superoxide formation. (**D**) Cardiac cytosolic oxidative stress was assessed by HPLC-based quantification of oxidized dihydrorhodamine 123 in murine heart tissue. The signal was normalized on the tissue wet weight. This assay mainly detects cytosolic superoxide and peroxynitrite formation (higher specificity for peroxynitrite). The data are mean ± SEM of 12-16 (**A**), 15-16 (**B**) and 3-4 (**C** and **D**) independent experiments. *, $p<0.05$ vs. old MnSOD-deficient mice (+/-).

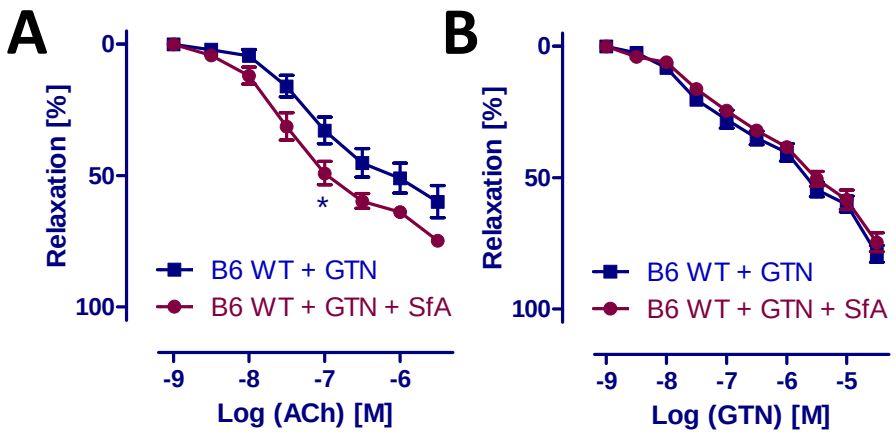

Supplemental Figure S6. Effects of mPTP inhibition by in vivo sanglifehrin A therapy on vascular function and cardiac oxidative stress in nitrate tolerant wild type mice. Vascular function was determined in aortic ring segments from nitrate tolerant mice (GTN, 16 µg/h for 4d) with or without sanglifehrin A (SfA) therapy (10 mg/kg/d). Isometric tension recordings were performed in response to endothelium-dependent (ACh, **A**) and endothelium-independent (GTN, **B**) vasodilators. The data are mean ± SEM of 7-8 independent experiments. *, $p<0.05$ vs. nitrate tolerant wild type mice.

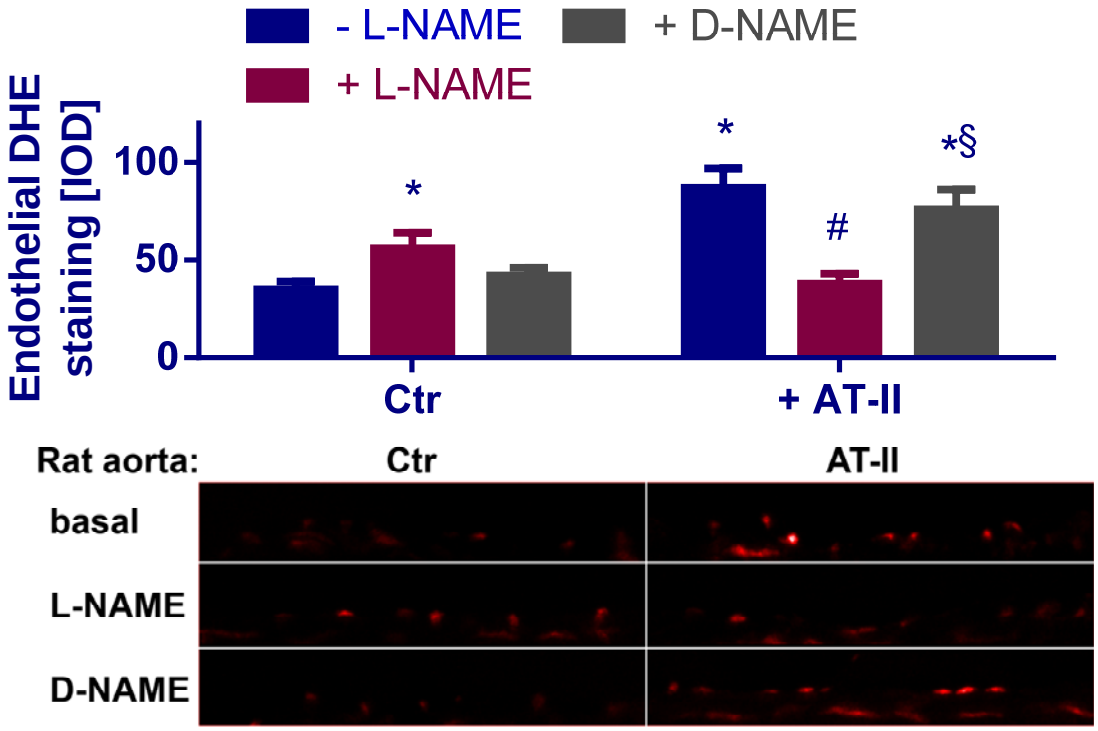

Supplemental Figure S7. Comparison of L-NAME versus D-NAME effects on endothelial superoxide formation in aorta from control and AT-II-infused rats. Rats were infused with AT-II (1 mg/kg/d for 7d) by implanted minipumps. The protocol was similar to the one for the mouse model (see Methods). (**B** and **C**) eNOS uncoupling was assessed by endothelial specific quantification of DHE fluorescence in aortic cryo sections that were either preincubated with L-NAME or D-NAME (each 500 µM) before embedding in Tissue Tek resin and cryo-sectioning. The eNOS inhibitor L-NAME increases the signal in the endothelial cell layer with functional eNOS (by suppression of the superoxide scavenger NO) and decreases the signal in endothelial cells with uncoupled eNOS (by inhibition of eNOS-derived superoxide formation). In contrast, the enantiomer D-NAME failed to induce similar effects supporting the specificity of the assay for eNOS-derived superoxide formation. Representative microscope images are shown below the densitometric quantifications (red=ROS and RNS (mainly superoxide) induced fluorescence). The pictures show the endothelial cell layer. *, $p<0.05$ vs. untreated control; $^{\#}$, $p<0.05$ vs. AT-II treatment; $^{\$}$, $p<0.05$ vs. untreated CypD$^{-/-}$ mice; §, $p<0.05$ vs. respective L-NAME group. The data are mean ± SEM of 5-7 independent experiments.

Extended Introduction

The starting point of our study was the mechanistic characterization of mtROS-triggered activation of the phagocytic oxidase in isolated human and murine leukocytes with various techniques and pharmacological inhibitors. We also assessed the impact of manganese superoxide dismutase (MnSOD, mitochondrial isoform of superoxide dismutase) or cyclophilin D (CypD, regulatory subunit of the mPTP) deficiency on cardiovascular complications in response to chronic angiotensin-II (AT-II) infusion in mice. Both animal models were not used in this context before and the use of the $CypD^{-/-}$ mice provides specific insight into the role of mPTP blockade whereas pharmacological inhibitors such as CsA and sanglifehrin A (SfA) have immunosuppressive side effects when used in vivo (for details see limitations of the study). The focus of these in vivo studies was to translate our in vitro findings to models of clinical relevance. We therefore used AT-II induced hypertension (high and low/subpressor dose) to study the effect of increased mitochondrial superoxide formation ($MnSOD^{+/-}$ mice) as well as genetic blockade of the mPTP on activation of leukocyte and cardiovascular NADPH oxidase as well as eNOS dysregulation/ uncoupling (e.g. by S-glutathionylation). As a second model of clinical relevance we studied the effect of the aging-process on this crosstalk and its adverse impact on eNOS and vascular function. In some settings the pharmacological inhibitor of the mPTP (SfA) was used in our mouse models of endothelial dysfunction.

Extended Results

Studies with old $MnSOD^{+/-}$ mice and nitrate tolerant mice

As a rescue, we performed in vivo cotherapy of the old MnSOD-deficient mice with the mPTP blocker sanglifehrin A resulting in a moderate improvement of endothelial function (ACh-response) but not endothelium–independent relaxation (GTN-response) (supplemental Fig. S5A and B). SfA prevents escape of mitochondrial superoxide, hydrogen peroxide and/or

peroxynitrite to the cytosol thereby ameliorating oxidative eNOS dysfunction in aged $MnSOD^{+/-}$ mice. In contrast, SfA does not significantly improve the mitochondrial superoxide, hydrogen peroxide and/or peroxynitrite levels in the matrix (mPTP blockade will keep these species in the matrix) and thereby fails to significantly improve the GTN-response, probably because ALDH-2 is still oxidatively inhibited. Likewise, cardiac membranous NADPH oxidase activity (measured by HPLC-based quantification of 2-HE) and release of peroxynitrite and/or superoxide (to a minor extent hydrogen peroxide) to the cytosol (determined by HPLC-based quantification of oxidized DHR 123) was improved by SfA therapy (supplemental Fig. S5C and D). Therefore, blockade of the mPTP obviously improved mtROS-triggered activation of NADPH oxidase and subsequent endothelial dysfunction in aged $MnSOD^{+/-}$ mice. Similar effects of SfA therapy were observed in nitrate tolerant mice in response to chronic nitroglycerin treatment: the ACh-response was improved whereas the GTN-response was not altered (supplemental Fig. S6).

Extended Discussion

During the last decade, AT-II induced vascular oxidative stress, endothelial dysfunction and hypertension in mice or rats was a frequently used model for mechanistic investigations on arterial hypertension in patients. The formation of superoxide was largely attributed to NADPH oxidases (14) and a number of studies using genetic deletion of NADPH oxidase subunits supported the essential role of this superoxide source for the pathogenesis of AT-II hypertension (11). A potential involvement of mitochondrial superoxide and hydrogen peroxide formation in this model was rather neglected. In 2005, Kimura et al. have shown that AT-II treatment leads to an opening of the mitochondrial ATP-sensitive potassium channels with subsequent loss in mitochondrial membrane potential and superoxide and hydrogen peroxide formation associated with mPTP opening and activation of redox-sensitive mitogen-activated protein (MAP) kinase (1,10). It was proposed that these AT-II effects mimic

ischemic preconditioning. More recently, Dikalov and coworkers have demonstrated that NADPH oxidase derived superoxide, hydrogen peroxide and/or peroxynitrite in response to AT-II stimulate mitochondrial oxidative stress contributing to overall AT-II dependent endothelial cell dysfunction (7). Even more important, a subsequent study from the same group demonstrated that AT-II-induced endothelial dysfunction and hypertension is significantly improved by cotherapy with mitochondria-targeted antioxidants or overexpression of MnSOD (the mitochondrial isoform of SODs) (6). These findings were also reviewed recently (3,5). In summary, these reports suggest that AT-II triggers a vicious circle involving mitochondria as an amplification mechanism for overall oxidative stress.

In 2007, Guzik et al. demonstrated a crucial role of immune cells to AT-II-triggered vascular oxidative stress, endothelial dysfunction and hypertension using mice lacking T and B cells (RAG-$1^{-/-}$ mice) (8). Adoptive transfer of T, but not B, cells restored these abnormalities. In a more recent study, Wenzel et al. extended these observations by establishing an important role of monocytes for the development of vascular complications in mice treated with AT-II by using a model with specific ablation of myelomonocytic cells (16). The important connection between the immune system, mtROS formation and AT-II-induced hypertension led us to test the following hypotheses: First, do mitochondrial superoxide and hydrogen peroxide activate phagocytic NADPH oxidase in white blood cells and may thereby contribute to AT-II-induced vascular complications? Second, does increased mitochondrial superoxide, hydrogen peroxide and subsequent peroxynitrite formation (e.g. by MnSOD deficiency) contribute to increased NADPH oxidase activity as well as to aggravated AT-II-mediated vascular complications? Third, is the mPTP opening an important constituent of the cascade that leads to mtROS triggered NADPH oxidase activation (e.g. by pharmacological inhibitors of mPTP CsA (in vitro) and SfA (in vivo) but more importantly, since no unspcific side effects with CypD deficiency)?

The reason for using isolated leukocytes in the present study to characterize the crosstalk between mitochondrial and Nox-derived ROS is based on the ratio between mitochondrial density and Nox activity in these cells. Leukocytes, especially neutrophils have a limited number of mitochondria as compared to other cells. Based on previous data/estimations there are 854 mitochondria/cell in blood mononuclear, 1111 in sperm, 2794 in muscle cells, 10800 in neurons and 25000 in liver cells (K.K. Singh [Birmingham, AL, USA] plenary lecture at the 18th Annual Meeting of the Society of Free Radical Biology and Medicine 2011, Atlanta, USA). In addition, leukocytes highly express the phagocytic NADPH oxidase (Nox2 isoform). These features make them particularly useful to study mtROS-induced NADPH oxidase activation, since the limited number of mitochondria will yield rather low levels of mtROS and the subsequent activation of NADPH oxidase will significantly amplify the overall ROS signal. This approach will avoid that mtROS signals outcompete the Nox-derived ROS signals.

Extended limitations

The present studies mainly concentrated on measurement of extracellular superoxide and hydrogen peroxide (both are present in isolated leukocytes). Intracellular measurements were restricted to Nox activity in membranous fractions (also superoxide), DHR123 oxidation which is most specific for peroxynitrite but also detects superoxide and finally protein tyrosine nitration (as an indirect read-out for peroxynitrite but also hydrogen peroxide/peroxidase activated nitrite). Since we can neither exclude formation of intracellular peroxynitrite from NO and superoxide nor its contribution to eNOS uncoupling and endothelial dysfunction and since it has been demonstrated that ROS and RNS contribute to redox signaling processes in the cytosol and mitochondria (4,9,12,13,15), we have sometimes used the generic term “ROS and RNS”, when not directly referring to a specific assay of our methods.

Extended references

1. Brandes RP. Triggering mitochondrial radical release: a new function for NADPH oxidases. *Hypertension* 45: 847-8, 2005.
2. Deng S, Kruger A, Kleschyov AL, Kalinowski L, Daiber A, Wojnowski L. Gp91phox-containing NAD(P)H oxidase increases superoxide formation by doxorubicin and NADPH. *Free Radic Biol Med* 42: 466-73, 2007.
3. Dikalov S. Cross talk between mitochondria and NADPH oxidases. *Free Radic Biol Med* 51: 1289-301, 2011.
4. Dikalov S, Griendling KK, Harrison DG. Measurement of reactive oxygen species in cardiovascular studies. *Hypertension* 49: 717-27, 2007.
5. Dikalov SI, Nazarewicz RR. Angiotensin II-Induced Production of Mitochondrial Reactive Oxygen Species: Potential Mechanisms and Relevance for Cardiovascular Disease. *Antioxid Redox Signal*.
6. Dikalova AE, Bikineyeva AT, Budzyn K, Nazarewicz RR, McCann L, Lewis W, Harrison DG, Dikalov SI. Therapeutic targeting of mitochondrial superoxide in hypertension. *Circ Res* 107: 106-16, 2010.
7. Doughan AK, Harrison DG, Dikalov SI. Molecular mechanisms of angiotensin II-mediated mitochondrial dysfunction: linking mitochondrial oxidative damage and vascular endothelial dysfunction. *Circ Res* 102: 488-96, 2008.
8. Guzik TJ, Hoch NE, Brown KA, McCann LA, Rahman A, Dikalov S, Goronzy J, Weyand C, Harrison DG. Role of the T cell in the genesis of angiotensin II induced hypertension and vascular dysfunction. *J Exp Med* 204: 2449-60, 2007.
9. Jamieson D, Chance B, Cadenas E, Boveris A. The relation of free radical production to hyperoxia. *Annu Rev Physiol* 48: 703-19, 1986.
10. Kimura S, Zhang GX, Nishiyama A, Shokoji T, Yao L, Fan YY, Rahman M, Abe Y. Mitochondria-derived reactive oxygen species and vascular MAP kinases: comparison of angiotensin II and diazoxide. *Hypertension* 45: 438-44, 2005.
11. Landmesser U, Cai H, Dikalov S, McCann L, Hwang J, Jo H, Holland SM, Harrison DG. Role of p47(phox) in vascular oxidative stress and hypertension caused by angiotensin II. *Hypertension* 40: 511-5, 2002.
12. Maghzal GJ, Krause KH, Stocker R, Jaquet V. Detection of reactive oxygen species derived from the family of NOX NADPH oxidases. *Free Radic Biol Med* 53: 1903-18, 2012.
13. Radi R, Cassina A, Hodara R, Quijano C, Castro L. Peroxynitrite reactions and formation in mitochondria. *Free Radic Biol Med* 33: 1451-64, 2002.
14. Rajagopalan S, Kurz S, Munzel T, Tarpey M, Freeman BA, Griendling KK, Harrison DG. Angiotensin II-mediated hypertension in the rat increases vascular superoxide production via membrane NADH/NADPH oxidase activation. Contribution to alterations of vasomotor tone. *Journal of Clinical Investigation* 97: 1916-23, 1996.
15. Ullrich V, Kissner R. Redox signaling: bioinorganic chemistry at its best. *J Inorg Biochem* 100: 2079-86, 2006.
16. Wenzel P, Knorr M, Kossmann S, Stratmann J, Hausding M, Schuhmacher S, Karbach SH, Schwenk M, Yogev N, Schulz E, Oelze M, Grabbe S, Jonuleit H, Becker C, Daiber A, Waisman A, Munzel T. Lysozyme M-positive monocytes mediate angiotensin II-induced arterial hypertension and vascular dysfunction. *Circulation* 124: 1370-1381, 2011.